The diatom Phaeodactylum tricornutum adjusts NPQ capacity in response to dynamic light via fine-tuned Lhcx and xanthophyll cycle pigment synthesis

Bernard Lepetit, Gautier Gélin, Mariana Lepetit, Sabine Sturm, Sascha Vugrinec, Alessandra Rogato, Peter G Kroth, Angela Falciatore, Johann Lavaud

The diatom *Phaeodactylum tricornutum* adjusts NPQ capacity in response to dynamic light via fine-tuned Lhcx and xanthophyll cycle pigment synthesis

Running title: NPQ capacity under dynamic light in *P. tricornutum*

Bernard Lepetit[1,2]*, Gautier Gélin[1], Mariana Lepetit[1], Sabine Sturm[2], Sascha Vugrinec[2], Alessandra Rogato[3,4], Peter G. Kroth[2], Angela Falciatore[5], Johann Lavaud[1,6]

[1] UMR7266 'LIENSs', CNRS Université de La Rochelle, Institut du littoral et de l'Environnement, 2 rue Olympe de Gouges, 17000 La Rochelle, France

[2] Zukunftskolleg, Pflanzliche Ökophysiologie, Universität Konstanz, 78457 Konstanz, Germany

[3] Institute of Biosciences and BioResources, CNR, Via P. Castellino 111, 80131 Naples, Italy

[4] Stazione Zoologica Anton Dohrn Villa Comunale 80121 Naples, Italy

[5] Sorbonne Universités, UPMC, Institut de Biologie Paris-Seine, CNRS, Laboratoire de Biologie Computationnelle et Quantitative, 15 rue de l'Ecole de Médecine, 75006 Paris, France

[6] UMI 3376 TAKUVIK, CNRS/Université Laval, Département de Biologie, Pavillon Alexandre-Vachon, 1045 avenue de la Médecine, Québec (Québec) G1V 0A6, Canada

*Corresponding author:

Bernard Lepetit
Zukunftskolleg, Pflanzliche Ökophysiologie, Universität Konstanz, 78457 Konstanz, Germany
E-mail: Bernard.Lepetit@uni-konstanz.de
Phone: +49 7531 883133

Total word count main body: 6485
Introduction word count: 1152
Materials and Methods word count: 1392
Results word count: 1651
Discussion word count: 1888
Conclusion word count: 261
Acknowledgement word count: 141
10 Figures, 5 Figures and 1 Table in the Supporting Information

Summary

- Diatoms contain a highly flexible capacity to dissipate excessively absorbed light by "Non-Photochemical fluorescence Quenching" (NPQ) based on the light induced conversion of diadinoxanthin (Dd) into diatoxanthin (Dt) and the presence of Lhcx proteins. Their NPQ fine regulation on the molecular level upon a shift to dynamic light conditions is unknown.
- We investigated the regulation of Dd+Dt amount, Lhcx gene and protein synthesis and NPQ capacity in the diatom *Phaeodactylum tricornutum* after a change from continuous low light to three days of sine (SL) or fluctuating (FL) light conditions. Four *P. tricornutum* strains with different NPQ capacities due to different expression of *Lhcx1* were included.
- All strains responded to dynamic light comparably, independently of initial NPQ capacity. During SL, NPQ capacity was strongly enhanced due to a gradual increase of Lhcx2 and Dd+Dt amount. During FL, cells enhanced their NPQ capacity at the first day due to increased Dd+Dt, Lhcx2 and Lhcx3; already at the second day light acclimation was accomplished. While quenching efficiency of Dt was strongly lowered during SL conditions, it remained high throughout the whole FL exposure.
- Our results highlight a more balanced and cost-effective photoacclimation strategy of *P. tricornutum* under FL than under SL conditions.

Keywords: diatoms, dynamic light, Lhcx, NPQ, *Phaeodactylum tricornutum*, photoprotection, xanthophyll cycle

Introduction

Diatoms are unicellular microalgae constituting one of the most important phytoplankton groups in terms of biodiversity (Mann & Vanormelingen, 2013) and productivity (about 45 % of marine carbon fixation) (Geider *et al.*, 2001). They strongly participate in the biological carbon pump and the functioning of contemporary aquatic ecosystems (Armbrust, 2009). Due to their high productivity and high lipid content, diatoms could potentially replace American fossil oil consumption in the future (Levitan *et al.*, 2014) or be used for production of high quality plastics (Roesle *et al.*, 2014). A peculiar feature of diatoms is their ability to live in turbulent waters, where they can benefit from high nutrient availabilities (Tozzi *et al.*, 2004). In such habitats light intensity changes over several orders of magnitude on the timescale of minutes (Long *et al.*, 1994; MacIntyre *et al.*, 2000; Lavaud, 2007), therefore flexible photosynthesis and efficient photoprotection mechanisms are necessary to avoid over-excitation of the photosynthetic apparatus which would lead to the generation of reactive oxygen species (ROS), eventually resulting in cell death (Niyogi & Truong, 2013). Diatoms possess both, an unusual flexibility of photosynthetic productivity (Wilhelm *et al.*, 2006; Kroth *et al.*, 2008; Lepetit *et al.*, 2012; Bailleul *et al.*, 2015), and effective photoprotection mechanisms which include: 1) a fast operating PSII electron cycle (Lavaud *et al.*, 2002c; Wagner *et al.*, 2016), 2) a tuneable amount of membrane dissolved xanthophylls diadinoxanthin (Dd) and diatoxanthin (Dt) acting as antioxidants (Lepetit *et al.*, 2010), and 3) a high capacity for dissipation of excess excitation energy, illustrated by non-photochemical fluorescence quenching (NPQ) (Lavaud & Goss, 2014). NPQ in plants and green algae is divided into three to four subtypes, which are not similarly well defined in diatoms (Lavaud & Goss, 2014; Goss & Lepetit, 2015). Here we will refer to NPQ as a photoprotective mechanism whose induction depends upon three regulatory components: (1) The proton gradient generated between the thylakoid lumen and the chloroplast stroma during light exposure (ΔpH), (2) a fast operating xanthophyll cycle (XC) through enzymatic conversion of Dd into Dt in the presence of the ΔpH and the back conversion in its absence (i.e. typically in the dark), and (3) chloroplast located, but nuclear encoded antenna proteins of the Light-Harvesting Complex (LHC) superfamily. While Lhcf proteins build up the peripheral light harvesting antenna (called "FCP", likely predominantly associated with PSII *in vivo*) (Grouneva *et al.*, 2011; Gundermann *et al.*, 2013; Nagao *et al.*, 2013; Schaller-Laudel *et al.*, 2015), Lhcr proteins form the PSI antenna (Veith *et al.*, 2009; Lepetit *et al.*, 2010; Grouneva *et al.*, 2011; Ikeda *et al.*, 2013; Bina *et al.*, 2016). In contrast, Lhcx proteins are involved in NPQ in the pennate diatom *Phaeodactylum tricornutum* (Bailleul *et al.*, 2010; Lepetit *et al.*,

2013) and the centric *Thalassiosira pseudonana* (Zhu & Green, 2010; Wu *et al.*, 2012; Dong *et al.*, 2015). Involvement of Lhcx proteins in photoprotection in other diatoms is also very likely (Beer *et al.*, 2006; Park *et al.*, 2010; Laviale *et al.*, 2015; Ghazaryan *et al.*, 2016). It is assumed that Lhcx proteins bind Dd and Dt (Beer *et al.*, 2006; Lepetit *et al.*, 2013) and they apparently influence the supramolecular organisation of the antenna complexes (Ghazaryan *et al.*, 2016). The location of Lhcx within thylakoids remains ambiguous as based on contrasting reports of both FCP (Beer *et al.*, 2006; Lepetit *et al*., 2010; Grouneva *et al.*, 2011; Nagao *et al.*, 2013; Schaller-Laudel *et al.*, 2015) and PSI association (Grouneva *et al.*, 2011). The current NPQ model proposes two major quenching sites in diatoms (Miloslavina *et al.*, 2009; Chukhutsina *et al.*, 2014, Lavaud & Goss, 2014; Derks *et al.,* 2015; Goss & Lepetit, 2015): Quenching site 1 is mechanistically independent of Dt (Chukhutsina *et al*., 2014) and is formed rapidly mainly by detached, oligomeric antenna complexes due to the build-up of the ΔpH, while quenching site 2 is located close to the PSII reaction centres and is directly dependent on Dt formation. Quenching site 1 also exists in *P. tricornutum* (Miloslavina *et al*., 2009), but in this species NPQ always relies on Dt (Lavaud *et al.*, 2002a; Goss *et al*., 2006), except under special (i.e. artificial) conditions (Lavaud & Kroth, 2006; Eisenstadt *et al.*, 2008; Lepetit et al., 2013). This apparent contradiction could not been fully solved so far, but an indirect influence of Dt also on formation of quenching site 1 has been postulated (Lavaud & Goss, 2014; Goss & Lepetit, 2015).

In different diatoms, the NPQ capacity, in relation to the light environment of the respective planktonic and benthic habitat, can be rather variable. Diatoms that cope with sudden light exposures, e.g. coastal planktonic and immotile estuarine sediment-inhabiting diatoms, show a higher NPQ capacity than diatoms living in more stable water bodies (e.g. semi-enclosed bays, open ocean) and the motile and photophobic sediment-inhabiting forms (Lavaud *et al.*, 2007; Dimier *et al.*, 2009; Barnett *et al.*, 2015). The same holds true for diatom species adapted to the seasonally successive polar habitats (Petrou *et al.*, 2011). *P. tricornutum* is cosmopolitan, but prefers habitats where light climate is unstable and reaches punctual but regular high intensities, such as coasts, estuaries, or rocky pools (De Martino *et al.*, 2007). Different *P. tricornutum* ecotypes have different and variable NPQ capacities (Lavaud & Lepetit, 2013) that largely depend on the amount of Lhcx1 (Bailleul *et al.*, 2010). Additionally, there is growing evidence that two other light regulated isoforms, Lhcx2 and Lhcx3, may also participate to NPQ under prolonged light stress (Lepetit *et al.*, 2013; Taddei *et al.*, 2016).

For several diatom species the influence of near-natural light conditions on the photosynthetic performance and on growth has been thoroughly investigated (Kromkamp & Limbeek, 1993; Litchman, 2000; Fietz & Nicklisch, 2002; Wagner *et al.*, 2006; Jakob *et al.*, 2007; van de Poll *et al.*, 2007; Kropuenske *et al.*, 2009; Su *et al.*, 2012; Jallet *et al.*, 2016). As *P. tricornutum* is one of the best characterized diatoms on the molecular level, we investigated its photophysiology during acclimation from stable low light to dynamic and potentially stressful light conditions with respect to the interplay between Dd+Dt synthesis, Lhcx expression and NPQ capacity. Sine light (SL) conditions simulated the rise and decline of the sun during a cloudless day in a stable water body. Fluctuating light conditions (FL) superimposed the effect of vertical cell movement along the water column in an idealized manner with a mixing from and to the aphotic zone via the surface within periods of 30 minutes. We also aimed at investigating the influence of the initial photoprotection capacity on the adjustment of NPQ capacity to dynamic light. Therefore, we used two *P. tricornutum* ecotypes with different initial NPQ capacities (i.e. low and high natural NPQ phenotypes, see Bailleul *et al.*, 2010), but also strains with silenced or overexpressed *Lhcx1* protein. Our results contribute to the better understanding of the molecular fine-tuning of NPQ capacity during acclimation to dynamic light conditions in pennate diatoms.

Materials and Methods

Cell culturing and light treatments

Experiments were performed in four *Phaeodactylum tricornutum* strains with different NPQ capacities: (1) *P. tricornutum* strain 1 (Pt1, CCAP 1055/1); (2) Pt1sil; Pt1 strain which contains an antisense construct against the *Lhcx1* gene, leading to reduced Lhcx1 protein synthesis (Bailleul *et al.*, 2010); (3) *P. tricornutum* strain 4 (Pt4, UTEX 646); (4) Pt4ov; Pt4 strain which overexpresses the *Lhcx1* gene. The full length cDNA of the *Lhcx1* gene (JGI ID: 27278) was cloned downstream of the *FcpA (Lhcf1)* promoter into the pPha-T1 transformation vector (Zaslavskaia *et al.*, 2000). Pt4 cells were biolistically transformed with this construct according to Kroth (2007). Positive clones were selected on Zeocin^{TM} containing solid medium plates. *Lhcx1* overexpressing clones were screened based on their NPQ capacity and amongst several clones showing increased NPQ capacity the one with the highest NPQ was selected for the present experiments (Pt4ov). This clone has an identical photosynthetic yield as the wildtype under low light conditions (data not shown), but shows

strongly increased *Lhcx1* gene expression (Fig. S1). All four strains were grown in airlift tubes (4 cm diameter) at 20°C in a 16 h day/8 h night rhythm with a light intensity of 50 µmol photons m^{-2} s^{-1} (onset at 8:00) defined as low light (LL). Light was provided by computer controlled flora LED units (CLF Plant Climatics, Germany) with all LEDs (white, blue, red and far red) switched on. Cells were cultured in sterile Provasoli's enriched F/2 seawater medium. Chlorophyll a (Chl a) concentration was determined as described in Lepetit *et al.* (2013). Cells in logarithmic phase were adjusted with fresh F/2 medium to a concentration of 1.4 µg Chl a mL^{-1} at 18:00 each day for four consecutive days. The 5^{th} day (day 0), sampling started (see "Sampling" below). The following three days (day 1 to day 3) two different dynamic light treatments were applied during the day phase, provided by the flora LED system: 1) SL with a maximum light intensity of 500 µmol photons m^{-2} s^{-1} reached at 16:00 (18.3 mol photons m^{-2} integrated daily light dose), 2) two different FL treatments with 32 light intervals in total, where maximum intensity was either 500 (FL 500, 4.5 mol photons m^{-2} integrated daily light dose) or 1000 µmol photons m^{-2} s^{-1} (FL 1000, 8.9 mol photons m^{-2} integrated daily light dose) (Fig. 1). Light intensities were measured with a spherical quantum sensor (US-SQS/L, Walz, Germany) in the centre of the airlift tubes. Due to the relatively large diameter of the airlift tubes and the relatively dense algal culture, light attenuation was steep, which, together with the bubbling of the cultures, led to a continuous micro-fluctuation superimposed on both SL and FL. The specific light intensities for all dynamic treatments are idealized and were calculated based on the formulas of Kroon *et al.* (1992) and as described in Wagner *et al.* (2006), assuming a dense algal culture during FL conditions with exponential light attenuation in the water column. During the whole experiment (day 0 to day 3), Chl a concentration was determined daily at 18:00 and cultures were diluted with fresh F/2 medium to a concentration of 1.4 µg Chl a mL^{-1}, in order to prevent nutrient limitation and self-shading.

Sampling

Cells were harvested with a sterile syringe via a tube drawn in the airlift flask which was sealed except for sampling. For pigment analyses, 500 µl of cells were filtered each day at 11:00, 14:00 and 17:00 on an Isopore Polycarbonate filter 1.2 µm (Millipore, USA) and immediately frozen in liquid nitrogen. Cells exposed to FL were additionally harvested during the light maxima directly before the three indicated time points. For gene expression and protein analyses, 15 and 23 mL of cell suspension, respectively, were harvested each day at 14:00 and centrifuged for 4 min at 4°C and 4000 g. The precipitated cells were resolved in 1

mL ice cooled phosphate buffered saline and centrifuged at 14000 g for 1 min. The pellet was frozen in liquid nitrogen and stored at -80 °C until further analysis.

Fluorescence analyses

Cells harvested each day at 11:00, 14:00 and 17:00 were acclimated to 30 µmol photons m^{-2} s^{-1} for 30 min before measuring the maximum photosynthetic efficiency of PSII as $(F_m-F_o)/F_m$ $=F_v/F_m$ with an Aqua Pen (PSI Instruments, Czech Republic). In order to take into account slower relaxing NPQ processes and to assess the maximum NPQ capacity, rapid light curves, measured with a Water PAM and an Imaging PAM (Walz, Germany), were recorded after 45 min acclimation to 30 µmol photons m^{-2} s^{-1}, by applying thirteen steps of increasing light intensity up to 1250 µmol m^{-2} s^{-1} with a respective duration of 30 s at 455 nm. Before the onset of the actinic light and during each rapid light curve, an 800 ms pulse of 4000 µmol photons m^{-2} s^{-1} was applied to determine the maximum fluorescence levels F_m and $F_{m'}$, respectively. Maximum relative electron transport rates ($rETR_{max}$) and other photosynthetic and photoprotective parameters were obtained by fitting the obtained values according to Eilers & Peeters (1988) and Serodio & Lavaud (2011). A description of these parameters can be found in Table S1.

Pigment, transcript and protein analyses

Pigment extraction and HPLC analysis were performed as described in Lepetit *et al.* (2013). The de-epoxidation state was calculated as DES = Dt/(Dd+Dt).

RNA extraction, cDNA synthesis, qPCR and quantification followed the protocol in Lepetit *et al.* (2013), except that *RPS* (ribosomal protein S1, JGI ID: 44451) was used as the reference gene instead of *18s* due to a more stable transcript amount under our dynamic light conditions. The primer sequences for *Lhcx1*, *Lhcx2* and *Lhcx3* are listed in Lepetit *et al.* (2013). For *RPS* we used 5'-AATTCCTCGAAGTCAACCAGG-3' and 5'-GTGCAAGAGACCGGACATAC-3' as forward and reverse primer, respectively, and for *Lhcf2* the forward and reverse primer were 5'-GCCGATATCCCCAATGGATTT-3' and 5'-CTTGGTCGAAGGAGTCCCATC-3', respectively.

Protein extraction and Western blot analysis followed the protocol described in Coesel *et al.* (2009), but using a 14% Lithiumdodecylsulfate PAGE for protein separation. Samples corresponding to an amount of 1 µg Chl a were loaded on the gel. Anti-FCP6 (Westermann & Rhiel, 2005) was kindly provided by Dr. Erhard Rhiel (University of Oldenburg, Germany). This antibody detects all Lhcx isoforms in *P. tricornutum* (Laviale *et al.*, 2015; Taddei *et al.*, 2016), but based on its sequence it has the highest affinity for Lhcx3 and the lowest affinity

for Lhcx2. Anti-FCP6 was applied in a 1:5000 dilution overnight. Accurate loading and blotting was verified by correct transfer of pre-stained protein markers (Roti-Mark BICOLOR, Roth, Germany) on the PVDF membrane (Amersham Hybond-P, GE Healthcare, USA), by staining gels with the Coomassie R-250 Pierce Imperial Protein stain (Thermo Fisher Scientific, USA) and by incubating the blot membrane with Anti-PsbB (CP47, Agrisera, Sweden). Anti-PsbB detection was only used as a proxy for correct loading and blotting, as the amount of CP47 has a high turnover under light stress conditions (Wu *et al.*, 2011). Antibody signals were detected using the ECL Plus chemiluminescence system (GE Healthcare, USA) followed by x-ray film exposure. In order to compare relative Lhcx protein expression within the time-course of the experiments, protein samples of each *P. tricornutum* strain of either the SL or the FL 1000 experiment were loaded on a single gel. Antibody signal intensities were quantified using ImageJ (http://imagej.nih.gov/ij/). For each blot several films with different exposure and development times were produced, in order to avoid the saturation of the immunodetection signal for Lhcx1 (due to its high abundance) and Lhcx3 (due to its highest affinity to the anti-FCP6), while also obtaining a signal for the weakly visible Lhcx2 protein (due to its lowest affinity to anti-FCP6). Relative quantification of Lhcx1 and Lhcx3 referred on the corresponding signal at unstressed conditions (day 0). As Lhcx2 could not be detected at day 0, relative quantification was performed based on comparison of Lhcx2 to the Lhcx3 value at day 0. For each experimental point (SL and FL 1000), the mean of all strains was calculated ,except that Pt4ov was omitted from the analysis of Lhcx1 expression due to its artificial regulation by the overexpressing *Lhcf1* promoter (see "*Cell culturing and light treatments"*).

Statistics

Significance with a P value ≤ 0.05 was determined with Student's t-test calculated with SigmaPlot, but for gene expression we used the Pairwise Fixed Reallocation Randomization Test performed by REST according to Pfaffl *et al.* (2002).

Results

NPQ capacity and photosynthetic parameters during SL and FL conditions

Before exposing cells to dynamic light conditions, we analysed their NPQ capacity under stable low light growth conditions. NPQ capacity was highest in the Lhcx1 overexpressing strain Pt4ov with values between 4 and 5 (Fig. 2, day 0). Pt1 showed an NPQ capacity of ~

2.5, Pt1sil of ~2 and Pt4 of ~1.8 (Fig. 2). These different NPQ capacities were mainly due to different expression of the *Lhcx1* gene (Fig. S1), as already shown in Bailleul *et al.* (2010). The very high NPQ capacity of the Pt4ov strain was achieved by driving *Lhcx1* gene expression by the *Lhcf1* promoter, resulting in a more than 10 fold higher *Lhcx1* transcript level (Fig. S1).

The rationale of working with *P. tricornutum* strains showing naturally or genetically-manipulated differential NPQ capacities was to investigate whether these differences would influence their acclimation to dynamic light conditions. There was a strong continuous rise of NPQ capacity during the SL treatment (except in Pt4ov, see below), while under FL conditions NPQ increased at the first day similarly as under SL conditions, but then slowed down (Fig. 2). Importantly, the high NPQ strains (Pt1 and Pt4ov) still exhibited the highest NPQ at the end of both dynamic light treatments. Pt4 eventually reached a higher or similar NPQ as Pt1sil under SL and FL conditions, respectively. The Pt4ov strain behaved somewhat differently, as there was no increase of NPQ on day 1 under SL. This is most likely due to the pronounced decrease of *Lhcx1* gene expression (Fig. S1), as its overexpressing *Lhcf1* promoter is repressed under light stress (Nymark *et al.*, 2009). However, from day 2 on Pt4ov also started to increase NPQ capacity. Interestingly, although under stable LL conditions (i.e. day 0) Pt4ov had already higher NPQ values than the other strains at the end of FL treatment, it further increased NPQ during FL exposure (Fig. 2). All these results did not indicate a strong influence of initial NPQ capacity on the NPQ adjustment to dynamic light; instead, all strains responded in a similar manner by increasing their NPQ capacity. As the standard errors were rather high due to the dynamic nature of the experiment, in the following we combined results of the different strains in order to better reveal the specific response of *P. tricornutum* to the very distinct dynamic light conditions. This way, it became directly apparent that the doubling of light intensity under FL 1000 conditions led to no further increase of NPQ compared to FL 500 conditions. Actually, with a final value of ~ 3.2 the NPQ was almost identical at both FL conditions, while it was 5.8 under SL conditions (Fig. 3).

The maximum photosynthetic yield of PSII gradually decreased during SL conditions, especially during day 3, to 0.55 (20 % decrease), illustrating the appearance of photoinhibition (Fig. 4a). In contrast, F_v/F_m was maintained high (~ 0.65) during FL conditions. Again, no differences between FL 500 and FL 1000 conditions were observed (data not shown, but can be seen from the minimal error bars in Fig. 4a). Because also no major differences between FL 500 and FL 1000 conditions could be observed during the

follow-up experiments, data were combined (unless otherwise noted), in order to highlight significant differences compared to SL.

Under SL conditions, $rETR_{max}$ (see Table S1 for the definition of the parameters) dropped during the first day and slightly increased over the next two days compared to LL (Fig. 4b). In contrast, $rETR_{max}$ did not change during the first day of FL, but strongly increased during day 2 and 3. α decreased by roughly 20 % already during the first day of SL and then stabilized (Fig. 4c). It didn't remarkably change under FL conditions. Interestingly, there was no major change in E_k between SL and FL conditions (Fig. 4d). It increased by ~ 50 % during day 2 and stabilized over day 3. The apparent low E_k values were likely due to the blue light of the Imaging-PAM excitation beam and are in line with previous E_k values obtained the same way (Serodio & Lavaud, 2011). Huge differences were observed in NPQ_{Ek}/NPQ_{max}. It increased from ~7 % in LL to almost 20 % under SL conditions, while under FL it even decreased (Fig. 4e). In line with this, also $E50_{NPQ}$ behaved differently: At first it decreased, but then increased under both conditions. However, while the final $E50_{NPQ}$ value under SL conditions was similar as under LL, it was more than 1.5 fold higher under FL conditions (Fig. 4f).

Pigment stoichiometry during SL and FL

The Chl a increase per day per culture volume (μ_{Chla}) strongly differed under both dynamic conditions. Under SL conditions, μ_{Chla} dramatically decreased by 50 % on day 1 (compared to LL) and by 80 % over the rest of the experiment (Fig. 5). In contrast, under FL conditions a slight decrease of μ_{Chla} occurred during the first day, while already from the second day on the cultures produced as much Chl a per day as during LL conditions. For both, the Chl c to Chl a and the Fx to Chl a ratio, no remarkable differences between SL and FL conditions could be observed (Fig. S2).

In general, changes of the NPQ capacity were well reflected by changes in the amount of XC pigments. Dd+Dt increased 3.4 fold during SL treatment, reaching its maximum on the last day (Fig. 6). Although most of the increase already occurred during day 1, the XC pool size steadily increased during day 2 and 3 with repeated drops at night. In contrast, under FL conditions the increase of XC pigments was only 1.7 fold, and the largest part of XC pigments was also synthesized on day 1. The observed trend was identical in all strains under both light conditions, although Pt1 strains synthesized more Dd+Dt than Pt4 strains (Fig. S3).

The DES (Dt/(Dd+Dt)) reached values of around 50 % during the first day of SL at 14:00 (6 hours after light onset) and 17:00 (9 hours after light onset) (Fig. S4). During the following

SL days and during all three days of FL conditions DES was lowest in the morning (11:00, 3 hours after light onset) and highest in the afternoon (17:00), in line with the respective light intensities). During the light intervals of FL conditions, DES reached similar values as under SL conditions, but always decreased below 10 % during the subsequent low light/dark phases, indicating that Dt epoxidation took place rapidly during the decline of light intensity.

NPQ versus Dd+Dt relationship

The ratio of NPQ *versus* Dd+Dt is a robust indicator for the efficiency of the XC pigments to confer NPQ (Lavaud & Lepetit, 2013; Lepetit *et al.*, 2013). NPQ/(Dd+Dt) strongly decreased during the first day of SL treatment and recovered during the following days (Fig. 7). At the last time point (day 3-17:00), it became statistically indistinguishable from day 0, indicating that eventually Dt quenching efficiency reached the levels of LL acclimated cells. In contrast, NPQ/(Dd+Dt) remained high under FL conditions, highlighting a high quenching efficiency of Dt. During the second and third day it was statistically supported even higher at some time points than under LL conditions.

Lhcx gene expression and protein synthesis

In agreement with previous analyses for low light to high light shifts (Nymark *et al.*, 2009; Lepetit *et al.*, 2013), cells of all *P. tricornutum* strains strongly increased the transcript amounts of *Lhcx2* and *Lhcx3* under both SL and FL conditions, while *Lhcx1* was only slightly more transcribed (Fig. S1; note that *Lhcx1* transcription in Pt4ov reacted differentially due to the regulation of the *Lhcx1* gene by the *Lhcf1* promoter). This became even more obvious, when comparing the mean values of all strains (Fig. 8a-c). Intriguingly, there was a strong difference in *Lhcx2* and *Lhcx3* transcript amounts depending on the light climate: Under SL conditions, *Lhcx2* transcription was much more pronounced than under FL. In contrast, *Lhcx3* transcript level was higher under FL conditions. Transcription of *Lhcx2* and *Lhcx3* increased throughout SL treatment, while under FL conditions the maximum transcript level was already reached on day 1 (but note the decrease of *Lhcx3* transcription on day 2 and 3). Lhcf2 is one of the major classical light harvesting antenna proteins of the FCP under low light conditions (Lepetit *et al.*, 2010; Grouneva *et al.*, 2011; Gundermann *et al.*, 2013), hence under stressful light conditions an expression pattern opposite to *Lhcx* genes was expected. Indeed, there was a strong *Lhcf2* transcript reduction throughout the whole SL treatment (Fig. 8d). In contrast, under FL conditions *Lhcf2* transcript levels dropped only during day 1, but reached almost initial levels already by day 2.

In order to investigate whether the differences in *Lhcx* transcription between SL and FL conditions were also reflected by the protein level, the Lhcx proteins were quantified. No significant changes could be observed for Lhcx1 compared to LL conditions neither in SL nor in FL (Fig. 9a). There was a gradual increase of Lhcx2 protein synthesis throughout the whole SL experiment (Fig. 9b and Fig. S5 for an example of the Western blots obtained for Pt4), while under FL conditions its level reached maximum values already on the second day and was much lower compared to SL conditions on day 2 and day 3. In contrast, Lhcx3 content similarly increased during day 1 under SL and FL, and declined during the following days (Fig. 9c). Hence, only the Lhcx2 protein content correlated with the respective amounts of transcripts, and both paralleled the increase in NPQ capacity under SL exposure (see Fig. 3). This is better illustrated by plotting the mean relative amount of Lhcx2 versus the mean increase of NPQ capacity under SL conditions of all strains (but Pt4ov due to its unusual NPQ behaviour caused by the Lhcx1 overexpressing *Lhcf1* promoter), yielding a linear correlation with an R^2 of 0.997 (Fig. 10).

Discussion

Up-regulation of NPQ capacity is independent of initial NPQ capacity during acclimation to dynamic light conditions

We could not observe major differences in adjustment of NPQ capacity during dynamic light conditions in the low NPQ strains (Pt1sil and Pt4) compared to the high NPQ strains (Pt1 and Pt4ov). In line with this result, there was also no correlation between initial NPQ capacity and XC pigment synthesis, the latter being strain dependent: Pt1 and Pt1sil showed a stronger increase of Dd+Dt pool size than Pt4ov and Pt4 (Fig. S3). Furthermore, the Pt4ov strain, which under LL already possessed an NPQ capacity as high as Pt1sil at the end of the SL treatment (Fig. 2), similarly increased *Lhcx2* and *Lhcx3* gene expression as well as the Dd+Dt pool size (Fig. S1 and Fig. S3). The apparently low influence of the initial NPQ capacity on the subsequent NPQ adjustment during dynamic light conditions may be due to the fact that initial NPQ capacity under stable LL conditions is first determined by Lhcx1 and Dd+Dt amount (Bailleul *et al.*, 2010). As reported here for dynamic light and before for prolonged high light conditions (Lepetit *et al.*, 2013), a higher NPQ capacity is obtained by the combined increase of Dd+Dt pool size and primarily Lhcx2 expression.

Insights into the regulation of NPQ actors in diatoms have been gained recently, and clearly photoreceptor mediated processes influence NPQ capacity (Schellenberger Costa *et al.*, 2013;

385 Brunet *et al.*, 2014). In line with this, the *Lhcx1* gene promoter has a binding motif for a blue
386 light receptor, aureochrome 1a (Schellenberger Costa *et al.*, 2013). The cryptochromes CPF
387 (Coesel *et al.*, 2009) and CryP (Juhas *et al.*, 2014) regulate expression of *Lhcx* genes.
388 Interestingly, in *Chlamydomonas reinhardtii* the cryptochrome aCRY, which is related to
389 CryP, seems to react rather on light intensity than on light quality (Beel *et al.*, 2012), hence
390 CryP could modulate NPQ capacity in diatoms in response to different light intensities.
391 Besides the influence of photoreceptors on NPQ adjustment, we previously demonstrated that
392 Dd+Dt increase and *Lhcx2* expression rates are controlled by changes in the redox state of the
393 PQ-pool, while Lhcx3 expression may be regulated via ROS (Lepetit *et al.*, 2013; Lepetit &
394 Dietzel, 2015). In the present study *Lhcx2* expression and Dd+Dt content correlated well
395 under both dynamic light conditions, indicating the presence of a common trigger. Clearly,
396 the expression of *Lhcx2* and *Lhcx3* differed under SL and FL, suggesting that both light
397 conditions elicit two different regulation pathways, which is likely due to the different
398 characteristics of SL and FL in combination with their different total light doses. The PQ-pool
399 redox state responsive *Lhcx2* and Dd+Dt reacted rather gradually to long lasting light stimuli
400 under SL, which generated a higher cumulative photon amount per day. In contrast, *Lhcx3*
401 expression was regulated by short but intense light intervals, conditions which are expected to
402 generate pronounced amounts of ROS. Because the NPQ capacity has an influence on energy
403 flow into the electron transport chain and thus on the redox state of the PQ-pool and on ROS
404 generation (Triantaphylidès *et al.*, 2008; Kruk & Szymańska, 2012), the concentration of the
405 reduced PQ-pool and ROS should be different in the four *P. tricornutum* strains under
406 dynamic light conditions. Still, the four strains adjusted their NPQ capacity in a similar way
407 under dynamic light conditions. The fact that NPQ capacity increases even in the highest NPQ
408 strain (Pt4ov) illustrates that initial NPQ capacity was not sufficient to avoid partial over-
409 reduction of the electron transport chain. Sensitive PQ-pool redox state and ROS responding
410 promoter elements may already react to a partly reduced PQ-pool and small amounts of ROS,
411 so that minor differences in these triggers would hardly differentially affect the expression of
412 *Lhcx* genes and the synthesis of Dd+Dt pigments. Moreover, the redox state of the PQ-pool
413 can be influenced by changes of the metabolome (Jungandreas *et al.*, 2014; Wilhelm *et al.*,
414 2014; Levitan *et al.*, 2015). Such influences would be fairly independent of the NPQ capacity
415 and could also explain the similar NPQ response in the four *P. tricornutum* strains.

416

Lhcx2 in combination with the amount of XC pigments likely increases NPQ capacity under dynamic light

In diatoms, the increase of XC pigments does not necessarily lead to a higher NPQ (Schumann *et al.*, 2007). Specific proteins must be synthesized to bind these pigments for an effective involvement in NPQ (Lepetit *et al.*, 2013). Lhcx1 does not increase significantly during dynamic light conditions (Fig. 9a), and hence confers only basal NPQ capacity. In Lhcx2 or Lhcx3 overexpression lines, both proteins provide additional NPQ capacity (Taddei *et al.*, 2016). Lhcx2 content similarly increased on day 1 in SL and FL conditions, and remained stable during the following days in FL, while it increased in SL. These features were paralleled by the NPQ capacity. In fact, Lhcx2 amount was linearly correlated to the NPQ capacity increase under SL conditions (Fig. 10). Although this correlation is based only on a few data points, it suggests Lhcx2 being a major actor in modelling NPQ capacity under dynamic light conditions, together with the size of the XC pigment pool and the degree of de-epoxidation.

The impact of Lhcx3 on NPQ capacity enhancement is difficult to deduce. Our data suggest that Lhcx3 was less responsible for NPQ increase during day 2 and 3 in SL and FL, as its protein content was rather decreasing (Fig. 9c). Instead, the prompt increase of Lhcx3 on day 1 under both dynamic conditions may provide a fast increase of photoprotection capacity, while Lhcx2 continues to add up during prolonged light stress conditions like under SL treatment. Interestingly, there was a significant difference in *Lhcx3* transcript levels between FL and SL on day 1, which was not reflected by the protein level. This suggests that posttranscriptional control mechanisms, that specifically respond to fast light intensity fluctuations, partially prevent Lhcx3 protein synthesis. In line with this, it was recently shown in *A. thaliana* that high light regulation of several high light responsive target proteins often occurs differentially on the transcriptional and translational level (Oelze *et al.*, 2014). An additional control point at the *Lhcx3* translational level might be a strategy to acclimate the NPQ system to an average light intensity delivered by light fluctuations, while keeping a high *Lhcx3* transcript reservoir in case of prolonged light stress. This would avoid a too strong down-regulation of photochemistry during low light periods, while ensuring sufficient excess energy dissipation during high light regular peak exposures, a feature in line with the fast on/off switch of the NPQ system (Lavaud *et al.*, 2007) and the fine regulation of Dd+Dt synthesis versus the velocity of light fluctuations (Giovagnetti *et al.*, 2014) in diatoms.

Besides Lhcx2, and to some extent Lhcx3, other proteins could contribute to additional NPQ capacity under dynamic light, especially to the slight increase of NPQ during FL on day 2 and

day 3. The *Lhcr* gene family contains a phylogenetically separated subclade (Nymark *et al.*, 2013), which genes are transcriptionally up-regulated during high light stress (Nymark *et al.*, 2009). The corresponding proteins may be at least partially involved in modulating NPQ capacity. Another possible candidate is Lhcf15, which is the only *Lhcf* gene showing up-regulation during short term light stress (Nymark *et al.*, 2009), but which especially responds to red light (Schellenberger Costa *et al.*, 2013; Valle *et al.*, 2014; Herbstová *et al.*, 2015). Lhcf15 can build up specific antennae complexes with a red-shifted fluorescence emission (Herbstová *et al.*, 2015), that could be correlated to the NPQ capacity (Lavaud & Lepetit, 2013).

FL triggers a very effective photoprotective response

Under SL conditions, the cells first synthesized much more Dd+Dt than could be used for NPQ. Eventually, the ratio NPQ/(Dd+Dt) was better adjusted towards a higher quenching efficiency of Dt due to a slowdown of Dd+Dt synthesis and a concomitant catch-up of Lhcx2 synthesis. Despite a strongly increased NPQ capacity as well as a massive reduction of Chl a synthesis and *Lhcf2* transcription, decrease in photosynthetic efficiency could not be completely prevented. In contrast, cells under FL conditions kept the NPQ/(Dd+Dt) efficiency rather comparable to that of LL conditions, i.e. they synthesized only as many Dd+Dt as actually could be used for providing an optimal effective involvement of Dt in NPQ. Parallel to enhancing NPQ capacity, FL cells adjusted the reactivity of NPQ activation. The light intensity, for which 50 % of the maximum NPQ capacity was reached, was shifted to much higher values (Fig. 4f). Simultaneously, despite increasing E_k, FL cells kept the level of NPQ activation at E_k very low (i.e. a few % of $NPQ_{max,}$ Fig. 4e). This is noteworthy, because although E_k increased similarly, SL cells were unable to adjust the threshold for NPQ onset and activated a pronounced NPQ already at E_k. Ultimately, FL cells strongly increased $rETR_{max}$, but kept α high as in LL cells, in line with previous results in *Skeletonema costatum* (Kromkamp & Limbeek, 1993). All these changes enabled FL cells to use absorbed light efficiently until E_k was reached and even beyond due to the moderate switch-on of NPQ. Hence, they exploited as much light as possible for photochemistry during the short light periods thanks to the adjustment of NPQ capacity and kinetics. Consequently, after one day of acclimation, μ_{Chla} and *Lhcf2* transcription reached similar values as under LL conditions. As FL cells developed a much higher NPQ capacity than LL cells, altogether FL acclimation does not correspond to either a low or high light type strategy, but shows peculiar

characteristics. Such special fluctuating light acclimation strategy has also been observed in the diatom *Stephanodiscus neoastraea* (Fietz & Nicklisch, 2002).

We have to note that the fine-acclimation to FL conditions with different intensity maximums may be limited. Although FL 1000 cells faced much higher light intensities, steeper light gradients and the double daily photon dose, NPQ capacity increased similarly as in FL 500 cells. On the one hand, this very similar NPQ pattern may be co-initiated by an internal trigger such as the circadian clock. The influence of the circadian clock on the regulation of the XC pigments in *P. tricornutum* has already been demonstrated (Ragni & d'Alcalà, 2007). On the other hand, Giovagnetti *et al.* (2014) showed that light acclimation response in *Pseudonitzschia multistriata* is triggered by light intensity, but also by the velocity of the light increase. Moreover, in *Skeletonema marinoi*, NPQ capacity is not directly correlated to the total daily photon dose (Orefice *et al.*, 2016). Our results suggest that, below a certain duration threshold of regular light periods, different high light intensities only trigger an efficient on/off reaction of NPQ capacity adjustment, but no fine-tuned response. This is possibly due to the lack of the gradual PQ-pool signal. Interestingly, when the light intervals become even shorter than the dark intervals in a fluctuating light regime, *P. tricornutum* is able to generate a very high NPQ (Lavaud *et al.*, 2002b; Ruban *et al.*, 2004), which may not be triggered by light, but may be elicited by darkness instead. As only the transcription of the *Lhcx4* isoform is stimulated in the dark (Lepetit *et al.*, 2013; Nymark *et al.*, 2013) and the respective protein can induce NPQ (Taddei *et al.*, 2016), Lhcx4, together with the increased Dd+Dt content (Lavaud *et al.*, 2002b), may be responsible for this particular increased NPQ capacity.

Conclusion

Our study highlights the importance of investigating the influence of dynamic light conditions on NPQ in diatoms. Recently, it was shown that *P. tricornutum* is coping well with fluctuating light conditions by possessing a low-cost PSII repair cycle compared to diatoms living in the open ocean in more stable light conditions (Lavaud *et al.*, 2016). A comprehensive study by Wagner *et al.* (2006) demonstrated that in *P. tricornutum* absorbed photons are converted to a much higher extent into biomass in FL than in SL conditions, which is due to a strongly decreased amount of alternative electrons and a lowered quantum requirement per molecule oxygen evolved. The finely adjusted regulation of NPQ capacity by balanced Lhcx2/Lhcx3 and Dd+Dt synthesis under FL has three consequences which support the observations of Wagner *et al.* (2006): (1) Investment costs for photoprotection

mechanisms are lower than in SL; (2) Photodamage is reduced, keeping costs for repair processes low; (3) Too much photoprotection, leading to a poor light energy to chemical energy conversion rate and hence to a high quantum requirement for carbon fixation, is prevented. This latter feature has been recently demonstrated to be of global importance in the upper ocean (Lin *et al.*, 2016). The better balanced photoacclimation strategy under FL compared to SL conditions may be one reason why diatoms dominate in habitats where the light climate is regularly punctuated with high intensity exposure periods, such as coastal waters and estuarine intertidal sediments (Strzepek & Harrison, 2004; Lavaud *et al.*, 2007; Dimier *et al.*, 2009; Petrou *et al.*, 2011; Barnett *et al.*, 2015).

Acknowledgement

We thank Dr. Torsten Jakob (Leipzig) for help with installing the dynamic light conditions, Doris Ballert (Konstanz) for performing the biolistic transformation of the Pt4ov strain, Dr. Erhard Rhiel (Oldenburg) for providing the FCP6 antibody and Dr. Giovanni Finazzi (Grenoble) for valuable scientific discussion. We also thank the three reviewers for their constructive criticism. This work was supported by the German Academic Exchange Service-DAAD (postdoctoral grant to B.L.), an Marie Curie Zukunftskolleg Incoming Fellowship, University of Konstanz (grant no. 291784, to B.L.), a University of Konstanz Zukunftskolleg Interim grant (to B.L.), the Centre National de la Recherche Scientifique and the French consortium Contrat de Plan État-Région Littoral (grants to J.L.), the Deutsche Forschungsgemeinschaft (grant nos. LE 3358/3-1 to B.L., LA–2368/2–1 to J.L., and KR–1661/7–1 to P.G.K.), and the Marie-Curie ITN CALIPSO (ITN 2013 GA 607607, to A.F.).

Author contribution

B.L., P.G.K., A.F. and J.L. designed research. B.L., G.G., M.L., S.S., S.V., A.R. and J.L. performed experiments. B.L. and J.L. analysed data. B.L., A.F. and J.L. interpreted results. B.L., A.R., P.G.K, A.F. and J.L. wrote the manuscript.

Reference list

Armbrust EV. 2009. The life of diatoms in the world's oceans. *Nature* **459**: 185-192.

Bailleul B, Berne N, Murik O, Petroutsos D, Prihoda J, Tanaka A, Villanova V, Bligny R, Flori S, Falconet D et al. 2015. Energetic coupling between plastids and mitochondria drives CO2 assimilation in diatoms. *Nature* **524**: 366-369.

Bailleul B, Rogato A, de Martino A, Coesel S, Cardol P, Bowler C, Falciatore A, Finazzi G. 2010. An atypical member of the light-harvesting complex stress-related protein family modulates diatom responses to light. *Proceedings of the National Academy of Sciences of the United States of America* **107**: 18214-18219.

Barnett A, Méléder V, Blommaert L, Lepetit B, Gaudin P, Vyverman W, Sabbe K, Dupuy C, Lavaud J. 2015. Growth form defines physiological photoprotective capacity in intertidal benthic diatoms. *The ISME journal* **9**: 32-45.

Beel B, Prager K, Spexard M, Sasso S, Weiss D, Müller N, Heinnickel M, Dewez D, Ikoma D, Grossman AR et al. 2012. A flavin binding cryptochrome photoreceptor responds to both blue and red light in *Chlamydomonas reinhardtii*. *The Plant Cell* **24**: 2992-3008.

Beer A, Gundermann K, Beckmann J, Büchel C. 2006. Subunit composition and pigmentation of fucoxanthin-chlorophyll proteins in diatoms: Evidence for a subunit involved in diadinoxanthin and diatoxanthin binding. *Biochemistry* **45**: 13046-13053.

Bína D, Herbstová M, Gardian Z, Vácha F, Litvín R. 2016. Novel structural aspect of the diatom thylakoid membrane: lateral segregation of photosystem I under red-enhanced illumination. *Scientific reports* **6**: 25583.

Brunet C, Chandrasekaran R, Barra L, Giovagnetti V, Corato F, Ruban AV. 2014. Spectral radiation dependent photoprotective mechanism in the diatom *Pseudo-nitzschia multistriata*. *PLoS One* **9**: e87015.

Chukhutsina VU, Büchel C, van Amerongen H. 2014. Disentangling two non-photochemical quenching processes in *Cyclotella meneghiniana* by spectrally-resolved picosecond fluorescence at 77K. *Biochimica et Biophysica Acta (BBA)-Bioenergetics* **1837**: 899-907.

Coesel S, Mangogna M, Ishikawa T, Heijde M, Rogato A, Finazzi G, Todo T, Bowler C, Falciatore A. 2009. Diatom PtCPF1 is a new cryptochrome/photolyase family member with DNA repair and transcription regulation activity. *Embo Reports* **10**: 655-661.

De Martino A, Meichenin A, Shi J, Pan K, Bowler C. 2007. Genetic and phenotypic characterization of *Phaeodactylum tricornutum* (Bacillariophyceae) accessions. *Journal of Phycology* **43**: 992-1009.

Derks A, Schaven K, Bruce D. 2015. Diverse mechanisms for photoprotection in photosynthesis. Dynamic regulation of photosystem II excitation in response to rapid environmental change. *Biochimica et Biophysica Acta (BBA)-Bioenergetics* **1847**: 468-485.

Dimier C, Giovanni S, Ferdinando T, Brunet C. 2009. Comparative ecophysiology of the xanthophyll cycle in six marine phytoplanktonic species. *Protist* **160**: 397-411.

Dong Y-L, Jiang T, Xia W, Dong H-P, Lu S-H, Cui L. 2015. Light harvesting proteins regulate non-photochemical fluorescence quenching in the marine diatom *Thalassiosira pseudonana*. *Algal Research* **12**: 300-307.

Eilers P, Peeters J. 1988. A model for the relationship between light intensity and the rate of photosynthesis in phytoplankton. *Ecological modelling* **42**: 199-215.

Eisenstadt D, Ohad I, Keren N, Kaplan A. 2008. Changes in the photosynthetic reaction centre II in the diatom *Phaeodactylum tricornutum* result in non-photochemical fluorescence quenching. *Environmental Microbiology* **10**: 1997-2007.

Fietz S, Nicklisch A. 2002. Acclimation of the diatom *Stephanodiscus neoastraea* and the cyanobacterium *Planktothrix agardhii* to simulated natural light fluctuations. *Photosynthesis Research* **72**: 95-106.

Geider RJ, Delucia EH, Falkowski PG, Finzi AC, Grime JP, Grace J, Kana TM, La Roche J, Long SP, Osborne BA et al. 2001. Primary productivity of planet earth: biological determinants and physical constraints in terrestrial and aquatic habitats. *Global Change Biology* **7**: 849-882.

Ghazaryan A, Akhtar P, Garab G, Lambrev PH, Büchel C. 2016. Involvement of the Lhcx protein Fcp6 of the diatom *Cyclotella meneghiniana* in the macro-organisation and structural flexibility of thylakoid membranes. *Biochimica et Biophysica Acta (BBA)-Bioenergetics* **1857**: 1373-1379.

Giovagnetti V, Flori S, Tramontano F, Lavaud J, Brunet C. 2014. The velocity of light intensity increase modulates the photoprotective response in coastal diatoms. *PLoS One* **9:** e103782.

Goss R, Lepetit B. 2015. Biodiversity of NPQ. *Journal of Plant Physiology* **172**: 13-32.

Goss R, Pinto EA, Wilhelm C, Richter M. 2006. The importance of a highly active and delta pH regulated diatoxanthin epoxidase for the regulation of the PSII antenna function in diadinoxanthin cycle containing algae. *Journal of Plant Physiology* **163**: 1008-1021.

Grouneva I, Rokka A, Aro EM. 2011. The thylakoid membrane proteome of two marine diatoms outlines both diatom-specific and species-specific features of the photosynthetic machinery. *Journal of Proteome Research* **10**: 5338-5353.

Gundermann K, Schmidt M, Weisheit W, Mittag M, Büchel C. 2013. Identification of several sub-populations in the pool of light harvesting proteins in the pennate diatom *Phaeodactylum tricornutum*. *Biochimica et Biophysica Acta (BBA) - Bioenergetics* **1827**: 303-310.

Herbstová M, Bína D, Koník P, Gardian Z, Vácha F, Litvín R. 2015. Molecular basis of chromatic adaptation in pennate diatom *Phaeodactylum tricornutum*. *Biochimica et Biophysica Acta (BBA) - Bioenergetics* **1847**: 534-543.

Ikeda Y, Yamagishi A, Komura M, Suzuki T, Dohmae N, Shibata Y, Itoh S, Koike H, Satoh K. 2013. Two types of fucoxanthin-chlorophyll-binding proteins I tightly bound to the photosystem I core complex in marine centric diatoms. *Biochimica et Biophysica Acta (BBA)-Bioenergetics* **1827:** 529-539.

Jakob T, Wagner H, Stehfest K, Wilhelm C. 2007. A complete energy balance from photons to new biomass reveals a light- and nutrient-dependent variability in the metabolic costs of carbon assimilation. *Journal of Experimental Botany* **58**: 2101-2112.

Jallet D, Caballero MA, Gallina AA, Youngblood M, Peers G. 2016. Photosynthetic physiology and biomass partitioning in the model diatom *Phaeodactylum tricornutum* grown in a sinusoidal light regime. *Algal Research* **18**: 51-60.

Juhas M, Zadow A, Spexard M, Schmidt M, Kottke T, Büchel C. 2014. A novel cryptochrome in the diatom *Phaeodactylum tricornutum* influences the regulation of light harvesting protein levels. *Febs Journal* **281:** 2299-2311.

Jungandreas A, Costa BS, Jakob T, von Bergen M, Baumann S, Wilhelm C. 2014. The acclimation of *Phaeodactylum tricornutum* to blue and red light does not influence the photosynthetic light reaction but strongly disturbs the carbon allocation pattern. *PLoS One* **9**: e99727.

Kromkamp J, Limbeek M. 1993. Effect of short-term variation in irradiance on light harvesting and photosynthesis of the marine diatom *Skeletonema costatum*: a laboratory study simulating vertical mixing. *Journal of general microbiology* **139**: 2277-2284.

Kroon BMA, Hes UM, Mur LR. 1992. An algal cyclostat with computer-controlled dynamic light regime. *Hydrobiologia* **238**: 63-70.

Kropuenske LR, Mills MM, van Dijken GL, Bailey S, Robinson DH, Welschmeyer NA, Arrigoa KR. 2009. Photophysiology in two major Southern Ocean phytoplankton taxa: photoprotection in *Phaeocystis antarctica* and *Fragilariopsis cylindrus*. *Limnology and Oceanography* **54**: 1176-1196.

Kroth PG. 2007. Genetic transformation - a tool to study protein targeting in diatoms. In: Van der Giezen M, ed. *Methods in Molecular Biology - Protein Targeting Protocols.* Totowa (New Jersey), USA: Humana Press, 257-268.

Kroth PG, Chiovitti A, Gruber A, Martin-Jezequel V, Mock T, Parker MS, Stanley MS, Kaplan A, Caron L, Weber T et al. 2008. A model for carbohydrate metabolism in the diatom *Phaeodactylum tricornutum* deduced from comparative whole genome analysis. *PLoS One* **3**: e1426.

Kruk J, Szymańska R. 2012. Singlet oxygen and non-photochemical quenching contribute to oxidation of the plastoquinone-pool under high light stress in Arabidopsis. *Biochimica et Biophysica Acta (BBA)-Bioenergetics* **1817**: 705-710.

Lavaud J. 2007. Fast regulation of photosynthesis in diatoms: mechanisms, evolution and ecopysiology. *Functional Plant Science and Biotechnology* **1**: 267-287.

Lavaud J, Goss R. 2014. The peculiar features of non-photochemical fluorescence quenching in diatoms and brown algae. In: Demmig-Adams B, Garab G, Adams III W, Govindjee, eds. *Non-Photochemical Quenching and Energy Dissipation in Plants, Algae and Cyanobacteria*. Dordrecht, The Netherlands: Springer, 421-443.

Lavaud J, Kroth PG. 2006. In diatoms, the transthylakoid proton gradient regulates the photoprotective non-photochemical fluorescence quenching beyond its control on the xanthophyll cycle. *Plant and Cell Physiology* **47**: 1010-1016.

Lavaud J, Lepetit B. 2013. An explanation for the inter-species variability of the photoprotective non-photochemical chlorophyll fluorescence quenching in diatoms. *Biochimica et Biophysica Acta (BBA) - Bioenergetics* **1827**: 294-302.

Lavaud J, Rousseau B, Etienne AL. 2002a. In diatoms, a transthylakoid proton gradient alone is not sufficient to induce a non-photochemical fluorescence quenching. *FEBS Letters* **523**: 163-166.

Lavaud J, Rousseau B, Van Gorkom HJ, Etienne AL. 2002b. Influence of the diadinoxanthin pool size on photoprotection in the marine planktonic diatom *Phaeodactylum tricornutum*. *Plant Physiology* **129**: 1398-1406.

Lavaud J, Six C, Campbell DA. 2016. Photosystem II repair in marine diatoms with contrasting photophysiologies. *Photosynthesis Research* **127**: 189-199.

Lavaud J, Strzepek RF, Kroth PG. 2007. Photoprotection capacity differs among diatoms: Possible consequences on the spatial distribution of diatoms related to fluctuations in the underwater light climate. *Limnology and Oceanography* **52**: 1188-1194.

Lavaud J, Van Gorkom HJ, Etienne AL. 2002c. Photosystem II electron transfer cycle and chlororespiration in planktonic diatoms. *Photosynthesis Research* **74**: 51-59.

Laviale M, Barnett A, Ezequiel J, Lepetit B, Frankenbach S, Méléder V, Serôdio J, Lavaud J. 2015. Response of intertidal benthic microalgal biofilms to a coupled light–temperature stress: evidence for latitudinal adaptation along the Atlantic coast of Southern Europe. *Environmental Microbiology* **117:** 3662-3677.

Lepetit B, Dietzel L. 2015. Light signaling in photosynthetic eukaryotes with 'green' and 'red' chloroplasts. *Environmental and Experimental Botany* **114**: 30-47.

Lepetit B, Goss R, Jakob T, Wilhelm C. 2012. Molecular dynamics of the diatom thylakoid membrane under different light conditions. *Photosynthesis Research* **111**: 245-257.

Lepetit B, Sturm S, Rogato A, Gruber A, Sachse M, Falciatore A, Kroth PG, Lavaud J. 2013. High light acclimation in the secondary plastids containing diatom *Phaeodactylum tricornutum* is triggered by the redox state of the plastoquinone pool. *Plant Physiology* **161**: 853-865.

Lepetit B, Volke D, Gilbert M, Wilhelm C, Goss R. 2010. Evidence for the existence of one antenna-associated, lipid-dissolved, and two protein-bound pools of diadinoxanthin cycle pigments in diatoms. *Plant Physiology* **154**: 1905-1920.

Levitan O, Dinamarca J, Hochman G, Falkowski PG. 2014. Diatoms: a fossil fuel of the future. *Trends in biotechnology* **32**: 117-124.

Levitan O, Dinamarca J, Zelzion E, Gorbunov MY, Falkowski PG. 2015. An RNA interference knock-down of nitrate reductase enhances lipid biosynthesis in the diatom *Phaeodactylum tricornutum*. *The Plant Journal* **84**: 963-973.

Lin H, Kuzminov FI, Park J, Lee S, Falkowski PG, Gorbunov MY. 2016. Phytoplankton. The fate of photons absorbed by phytoplankton in the global ocean. *Science* **351**: 264-267.

Litchman E. 2000. Growth rates of phytoplankton under fluctuating light. *Freshwater Biology* **44**: 223-235.

Long SP, Humphries S, Falkowski PG. 1994. Photoinhibition of Photosynthesis in Nature. *Annual Review of Plant Physiology and Plant Molecular Biology* **45**: 633-662.

MacIntyre HL, Kana TM, Geider RJ. 2000. The effect of water motion on short-term rates of photosynthesis by marine phytoplankton. *Trends in Plant Science* **5**: 12-17.

Mann DG, Vanormelingen P. 2013. An inordinate fondness? The number, distributions, and origins of diatom species. *Journal of Eukaryotic Microbiology* **60**: 414-420.

Nagao R, Takahashi S, Suzuki T, Dohmae N, Nakazato K, Tomo T. 2013. Comparison of oligomeric states and polypeptide compositions of fucoxanthin chlorophyll a/c-binding protein complexes among various diatom species. *Photosynthesis Research* **117**: 281-288.

Niyogi KK, Truong TB. 2013. Evolution of flexible non-photochemical quenching mechanisms that regulate light harvesting in oxygenic photosynthesis. *Current Opinion in Plant Biology* **16**: 307-314.

Nymark M, Valle KC, Brembu T, Hancke K, Winge P, Andresen K, Johnsen G, Bones AM. 2009. An integrated analysis of molecular acclimation to high light in the marine diatom *Phaeodactylum tricornutum*. *PLoS One* **4**: e7743.

Nymark M, Valle KC, Hancke K, Winge P, Andresen K, Johnsen G, Bones AM, Brembu T. 2013. Molecular and photosynthetic responses to prolonged darkness and subsequent acclimation to re-illumination in the diatom *Phaeodactylum tricornutum*. *PLoS One* **8**: e58722.

Oelze M-L, Muthuramalingam M, Vogel MO, Dietz K-J. 2014. The link between transcript regulation and de novo protein synthesis in the retrograde high light acclimation response of *Arabidopsis thaliana*. *BMC genomics* **15**: 320.

Orefice I, Chandrasekaran R, Smerilli A, Corato F, Caruso T, Casillo A, Corsaro MM, Dal Piaz F, Ruban AV, Brunet C. 2016. Light-induced changes in the photosynthetic physiology and biochemistry in the diatom *Skeletonema marinoi*. *Algal Research* **17**: 1-13.

Park S, Jung G, Hwang Ys, Jin E. 2010. Dynamic response of the transcriptome of a psychrophilic diatom, *Chaetoceros neogracile*, to high irradiance. *Planta* **231**: 349-360.

Petrou K, Doblin M, Ralph P. 2011. Heterogeneity in the photoprotective capacity of three Antarctic diatoms during short-term changes in salinity and temperature. *Marine Biology* **158**: 1029-1041.

Pfaffl MW, Horgan GW, Dempfle L. 2002. Relative expression software tool (REST) for group-wise comparison and statistical analysis of relative expression results in real-time PCR. *Nucleic Acids Research* **30**: e36.

Ragni M, d'Alcalà MR. 2007. Circadian variability in the photobiology of *Phaeodactylum tricornutum*: pigment content. *Journal of Plankton Research* **29**: 141-156.

Roesle P, Stempfle F, Hess SK, Zimmerer J, Río Bártulos C, Lepetit B, Eckert A, Kroth PG, Mecking S. 2014. Synthetic polyester from algae oil. *Angewandte Chemie International Edition* **53**: 6800-6804.

Ruban AV, Lavaud J, Rousseau B, Guglielmi G, Horton P, Etienne AL. 2004. The super-excess energy dissipation in diatom algae: comparative analysis with higher plants. *Photosynthesis Research* **82**: 165-175.

Schaller-Laudel S, Volke D, Redlich M, Kansy M, Hoffmann R, Wilhelm C, Goss R. 2015. The diadinoxanthin diatoxanthin cycle induces structural rearrangements of the isolated FCP antenna complexes of the pennate diatom *Phaeodactylum tricornutum*. *Plant Physiology and Biochemistry* **96:** *364-376.*

Schellenberger Costa B, Jungandreas A, Jakob T, Weisheit W, Mittag M, Wilhelm C. 2013. Blue light is essential for high light acclimation and photoprotection in the diatom *Phaeodactylum tricornutum*. *Journal of Experimental Botany* **64**: 483-493.

Schumann A, Goss R, Jakob T, Wilhelm C. 2007. Investigation of the quenching efficiency of diatoxanthin in cells of *Phaeodactylum tricornutum* (Bacillariophyceae) with different pool sizes of xanthophyll cycle pigments. *Phycologia* **46**: 113-117.

Serôdio J, Lavaud J. 2011. A model for describing the light response of the nonphotochemical quenching of chlorophyll fluorescence. *Photosynthesis Research* **108**: 61-76.

Strzepek RF, Harrison PJ. 2004. Photosynthetic architecture differs in coastal and oceanic diatoms. *Nature* **431**: 689-692.

Su W, Jakob T, Wilhelm C. 2012. The impact of nonphotochemical quenching of fluorescence on the photon balance in diatoms under dynamic light conditions. *Journal of Phycology* **48**: 336-346.

Taddei L, Stella GR, Rogato A, Bailleul B, Fortunato AE, Annunziata R, Lepetit B, Lavaud J, Bouly J-P, Finazzi G et al. 2016. Multi-signal control of the expression of the LHCX protein family in the marine diatom *Phaeodactylum tricornutum*. *Journal of Experimental Botany* **67**: 3939-3951.

Tozzi S, Schofield O, Falkowski P. 2004. Historical climate change and ocean turbulence as selective agents for two key phytoplankton functional groups. *Marine Ecology Progress Series* **274**: 123-132.

Triantaphylidès C, Krischke M, Hoeberichts FA, Ksas B, Gresser G, Havaux M, Van Breusegem F, Mueller MJ. 2008. Singlet oxygen is the major reactive oxygen species involved in photooxidative damage to plants. *Plant Physiology* **148**: 960-968.

Valle KC, Nymark M, Aamot I, Hancke K, Winge P, Andresen K, Johnsen G, Brembu T, Bones AM. 2014. System responses to equal doses of photosynthetically usable radiation of blue, green, and red light in the marine diatom *Phaeodactylum tricornutum*. *PLoS One* **9**: e114211.

van de Poll WH, Visser RJW, Buma AGJ. 2007. Acclimation to a dynamic irradiance regime changes excessive irradiance sensitivity of *Emiliania huxleyi* and *Thalassiosira weissflogii*. *Limnology and Oceanography* **52**: 1430-1438.

Veith T, Brauns J, Weisheit W, Mittag M, Büchel C. 2009. Identification of a specific fucoxanthin-chlorophyll protein in the light harvesting complex of photosystem I in the diatom *Cyclotella meneghiniana*. *Biochimica et Biophysica Acta-Bioenergetics* **1787**: 905-912.

Wagner H, Jakob T, Lavaud J, Wilhelm C. 2016. Photosystem II cycle activity and alternative electron transport in the diatom *Phaeodactylum tricornutum* under dynamic light conditions and nitrogen limitation. *Photosynthesis Research* **128**: 151-161.

Wagner H, Jakob T, Wilhelm C. 2006. Balancing the energy flow from captured light to biomass under fluctuating light conditions. *New Phytologist* **169**: 95-108.

Westermann M, Rhiel E. 2005. Localisation of fucoxanthin chlorophyll a/c-binding polypeptides of the centric diatom *Cyclotella cryptica* by immuno-electron microscopy. *Protoplasma* **225**: 217-223.

Wilhelm C, Büchel C, Fisahn J, Goss R, Jakob T, LaRoche J, Lavaud J, Lohr M, Riebesell U, Stehfest K et al. 2006. The regulation of carbon and nutrient assimilation in diatoms is significantly different from green algae. *Protist* **157**: 91-124.

Wilhelm C, Jungandreas A, Jakob T, Goss R. 2014. Light acclimation in diatoms: From phenomenology to mechanisms. *Marine genomics* **16**: 5-15.

Wu H, Cockshutt AM, McCarthy A, Campbell DA. 2011. Distinctive photosystem II photoinactivation and protein dynamics in marine diatoms. *Plant Physiology* **156**: 2184-2195.

Wu H, Roy S, Alami M, Green B, Campbell DA. 2012. Photosystem II photoinactivation, repair and protection in marine centric diatoms. *Plant Physiology* **160**: 464-476.

Zaslavskaia LA, Lippmeier JC, Kroth PG, Grossman AR, Apt KE. 2000. Transformation of the diatom *Phaeodactylum tricornutum* (Bacillariophyceae) with a variety of selectable marker and reporter genes. *Journal of Phycology* **36**: 379-386.

Zhu SH, Green BR. 2010. Photoprotection in the diatom *Thalassiosira pseudonana*: Role of LI818-like proteins in response to high light stress. *Biochimica et Biophysica Acta (BBA)-Bioenergetics* **1797**: 1449-1457.

Figure legends

Figure 1: Dynamic light conditions used in the experiments. One sine light (SL) and two fluctuating light (FL) conditions with different intensities were applied during the daily phases of the light exposure and light intensity was measured every minute.

Figure 2: Comparison of NPQ capacity in the four different *Phaeodactylum tricornutum* strains (Pt1, Pt1sil, Pt4, Pt4ov) under SL (**a**) and FL (**b**) conditions. Time is indicated as experimental day (0 to 3, separated with vertical bars/arrow) and the respective time of sampling. Dynamic light conditions started on day 1 (indicated with an arrow). FL values combine data from the FL 500 and FL 1000 treatment. Values represent the means ± SE of three to four different experiments.

Figure 3: Mean NPQ values of *Phaeodactylum tricornutum* strains Pt1, Pt1sil and Pt4 under SL and FL conditions. Pt4ov was not included in the mean due to its much higher NPQ and its partly unusual characteristics (cf. Fig. 2); this is exemplified by its SL 500 trace (dashed line). Time is indicated as experimental day (0 to 3, separated with vertical bars/arrow) and the respective time of sampling. Dynamic light conditions started on day 1 (indicated with an arrow). Values represent the means ± SE of at least six biological replicates (except Pt4ov-SL 500: three biological replicates).

Figure 4: Mean photosynthetic and photoprotective parameters of all four *Phaeodactylum tricornutum* strains under SL and FL (500 and 1000 combined) conditions. a) Fv/Fm; b) the maximum relative electron transport rate ($rETR_{max}$); c) α, the slope of the relative electron transport rate versus light intensity under non-saturating light conditions; d) E_k, the interception point between α and ETR_{max}, a measure for the minimal light intensity to saturate photosynthesis; e) NPQ_{Ek}/NPQ_{max}, indicates the relative amount of NPQ at E_k; f) E_{50}, the light intensity, at which half of NPQ_{max} capacity is reached. Time is indicated as experimental day (0 to 3, separated with vertical bars/arrow) and the respective time of sampling. Dynamic light conditions started on day 1 (indicated with an arrow). Values represent the means ± SE of at least eight biological replicates. Meaning of statistical significance letters: a, values are significantly different compared to day 0 ($p < 0.05$); b, values from cells exposed to FL are significantly different compared to cells exposed to SL for the same time point ($p < 0.05$).

Figure 5: Chl a increase rate per day per culture volume (μ_{Chla}) of all four *Phaeodactylum tricornutum* strains under SL and FL 1000 conditions. Dynamic light conditions started on day 1 (indicated with an arrow). μ_{Chla} (in day^{-1}) was calculated as $\mu_{Chla} = \ln (Chl\ t_n/1.4)$, where

Chl t_n refers to the Chl a content measured at 18:00 during the four days of experiment (day 0 to day 3) and 1.4 is the Chl a content (in µg mL^{-1}) at which the cultures were adjusted to each day after Chl a determination. Because data for FL 500 conditions were not complete they were omitted, but, similarly to FL 1000 cells, FL 500 cells showed a higher μ_{Chla} than SL 500 cells. Values represent the means ± SE of at least four biological replicates. Meaning of significance letters: a, μ_{Chla} is significantly different compared to day 0 ($p < 0.05$); b, μ_{Chla} is significantly different in cells exposed to FL 1000 conditions compared to cells exposed to SL conditions for the same day ($p < 0.05$).

Figure 6: Mean diadinoxanthin and diatoxanthin (Dd+Dt) pool size (in mol (100 mol Chl a)$^{-1}$) of all four *Phaeodactylum tricornutum* strains under SL and FL (500 and 1000 combined) conditions. Time is indicated as experimental day (0 to 3, separated with vertical bars/arrow) and the respective time of sampling. Dynamic light conditions started on day 1 (indicated with an arrow). For SL conditions, data for each strain are available in Fig. S4. Values represent the means ± SE of eight biological replicates. Meaning of statistical significance letters: a, Dd+Dt pool size is significantly different compared to day 0 at 17:00 ($p < 0.05$); b, Dd+Dt pool size from cells exposed to the respective FL light treatment is significantly different compared to cells exposed to SL for the same time point ($p < 0.05$).

Figure 7: Correlation of NPQ capacity versus Dd+Dt (in mol (100 mol Chl a)$^{-1}$) under SL and FL (500 and 1000 combined) conditions. Values are taken from all *Phaeodactylum tricornutum* strains except Pt4ov due to its different characteristics in NPQ (cf. Fig. 2). Time is indicated as experimental day (0 to 3, separated with vertical bars/arrow) and the respective time of sampling. Dynamic light conditions started on day 1 (indicated with an arrow). Values represent the means ± SE of six biological replicates. Meaning of statistical significance letters: a, NPQ/(Dd+Dt) is significantly different compared to day 0 at 17:00 ($p < 0.05$); b, NPQ/(Dd+Dt) from cells exposed to FL is significantly different compared to cells exposed to SL for the same time point ($p < 0.05$).

Figure 8: Relative transcript amounts of *Lhcx1* (**a**), *Lhcx2* (**b**), *Lhcx3* (**c**) and *Lhcf2* (**d**) under SL and FL (500 and 1000 combined) conditions. Gene expression was normalized on transcript amount of the *RPS* gene. For each gene, the expression was calculated as the mean transcript amount of all *Phaeodactylum tricornutum* strains at the specific time points and light conditions except for *Lhcx1* where the values of Pt4ov were omitted due to the artificial *Lhcf1* promoter in this strain (c.f. Fig. S1). Dynamic light conditions started on day 1 (indicated with an arrow). Values represent the means ± SE of eight biological replicates

(except for Lhcx1 with six biological replicates), and each biological replicate was measured in technical triplicates. Meaning of significance letters: a, Gene is significantly differentially expressed compared to day 0 ($p < 0.05$); b, Gene from cells exposed to FL is significantly differentially expressed compared to cells at the corresponding time point exposed to SL ($p < 0.05$).

Figure 9: Mean of relative protein expression of Lhcx1 (**a**), Lhcx2 (**b**) and Lhcx3 (**c**) of all *Phaeodactylum tricornutum* strains under SL and FL 1000 conditions, respectively. For Lhcx1, protein expression data of Pt4ov were omitted due to the artificial regulation by the *Lhcf1* promoter (c.f. Fig. S1). Dynamic light conditions started on day 1 (indicated with an arrow). Values represent the means ± SE of at least four biological replicates (except for Lhcx1 with at least three biological replicates). Meaning of significance letters: a, protein is significantly differentially expressed compared to day 0 ($p < 0.05$); b, protein from cells exposed to FL is significantly differentially expressed compared to cells at the corresponding time point exposed to SL ($p < 0.05$).

Figure 10: Correlation of relative Lhcx2 protein content *versus* NPQ increase under SL conditions. NPQ was calculated as $NPQ_{day1,2,3} - NPQ_{day\ 0}$, always measured at the 14:00 time point. The three data points correspond to the Lhcx2 protein amount *versus* NPQ on day 1, day 2 and day 3. Values for NPQ and Lhcx2 protein content are the means ± SE of all *Phaeodactylum tricornutum* strains except Pt4ov.

Supporting information (SI) can be found in a separate sheet. It contains:

Table S1: Photophysiological parameters used in this study

Fig. S1: Transcript levels of *Lhcx1* - *Lhcx3* and *Lhcf2* genes under SL and FL conditions in all four *P. tricornutum* strains

Fig. S2: Fx/Chl a and Chl c/Chl a content of all four *P. tricornutum* strains under SL and FL conditions

Fig. S3: Dd+Dt pool size in the four individual *P. tricornutum* strains during SL and FL conditions

Fig. S4: De-epoxidation state of all four *P. tricornutum* strains under SL and FL conditions

Fig. S5: Lhcx protein expression in Pt4 during SL and FL conditions

Figures

Lepetit et al., Fig. 1

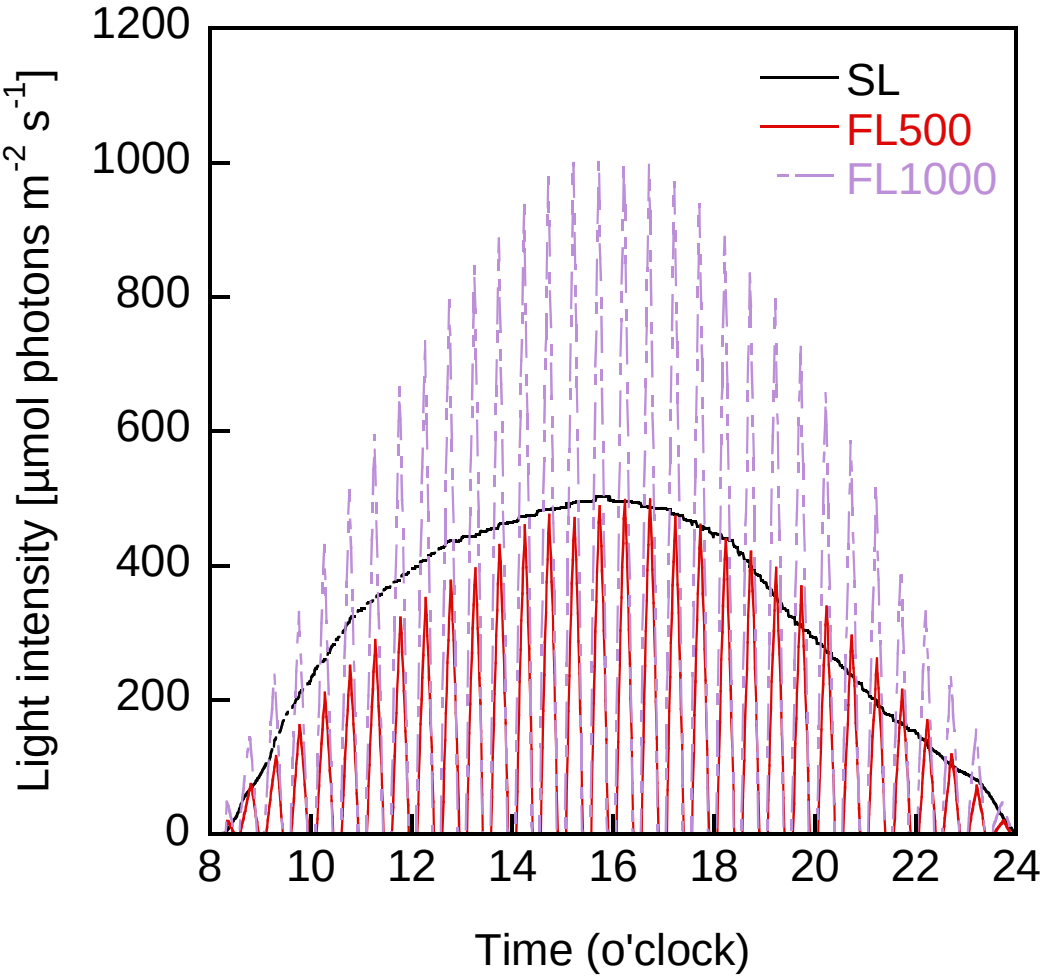

Lepetit et al., Fig. 2

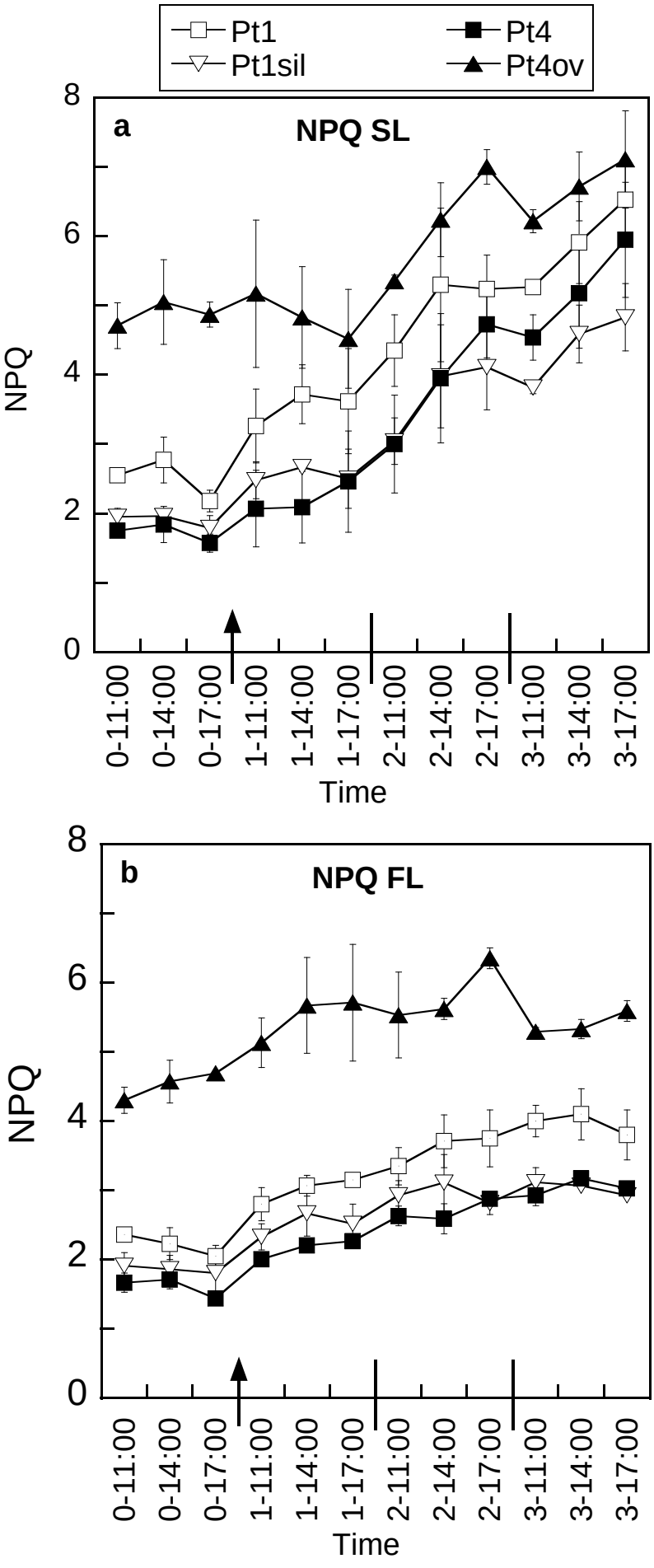

Lepetit et al., Fig. 3

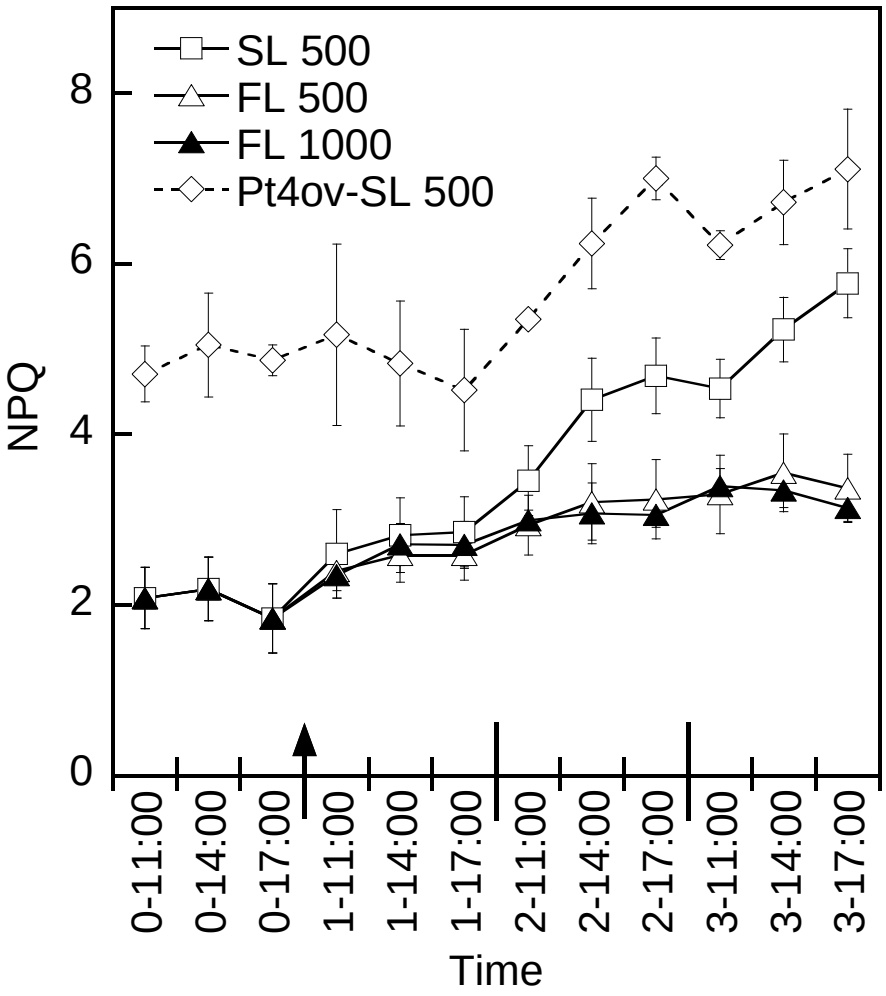

Lepetit et al. Fig. 4

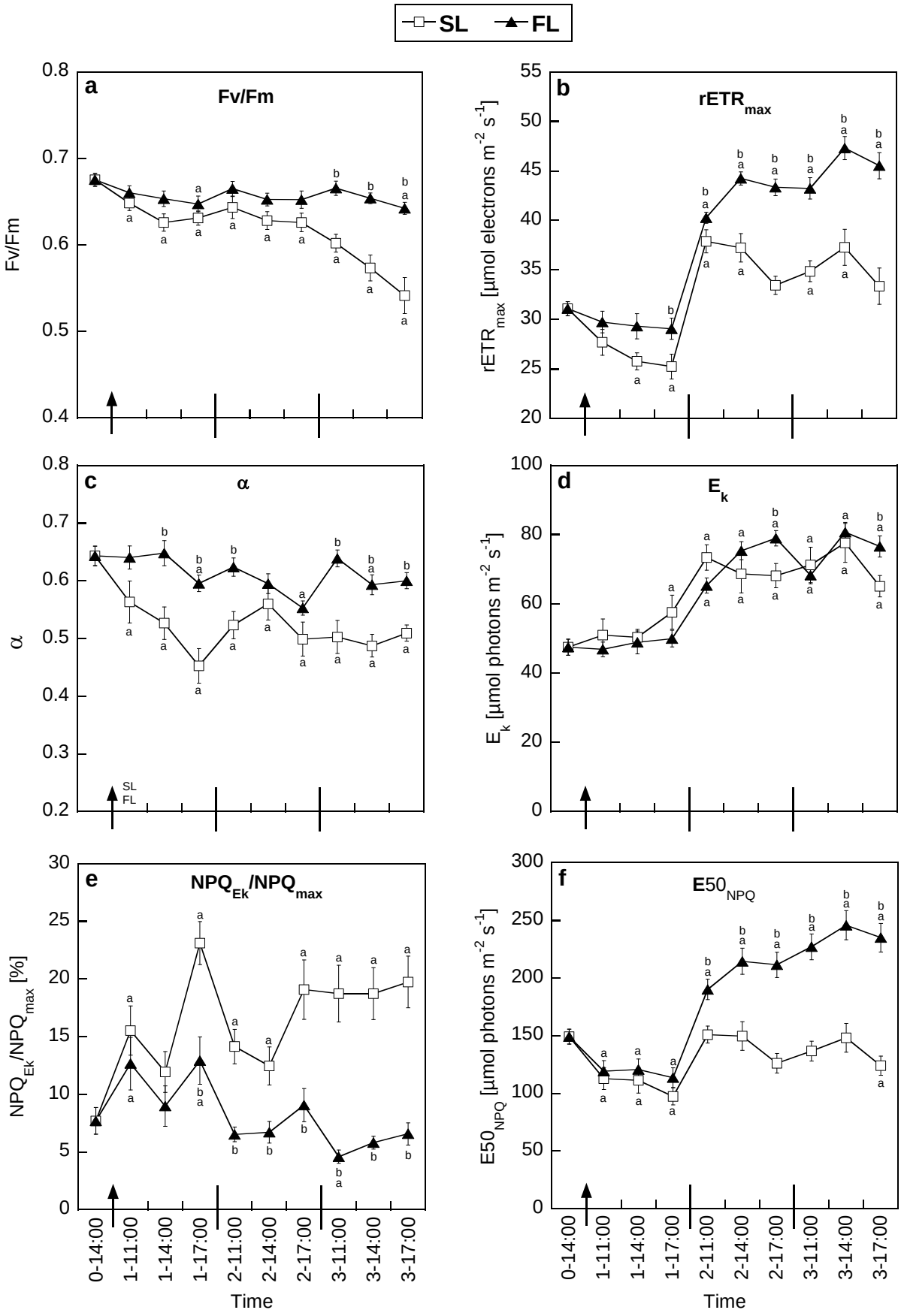

Lepetit et al., Fig. 5

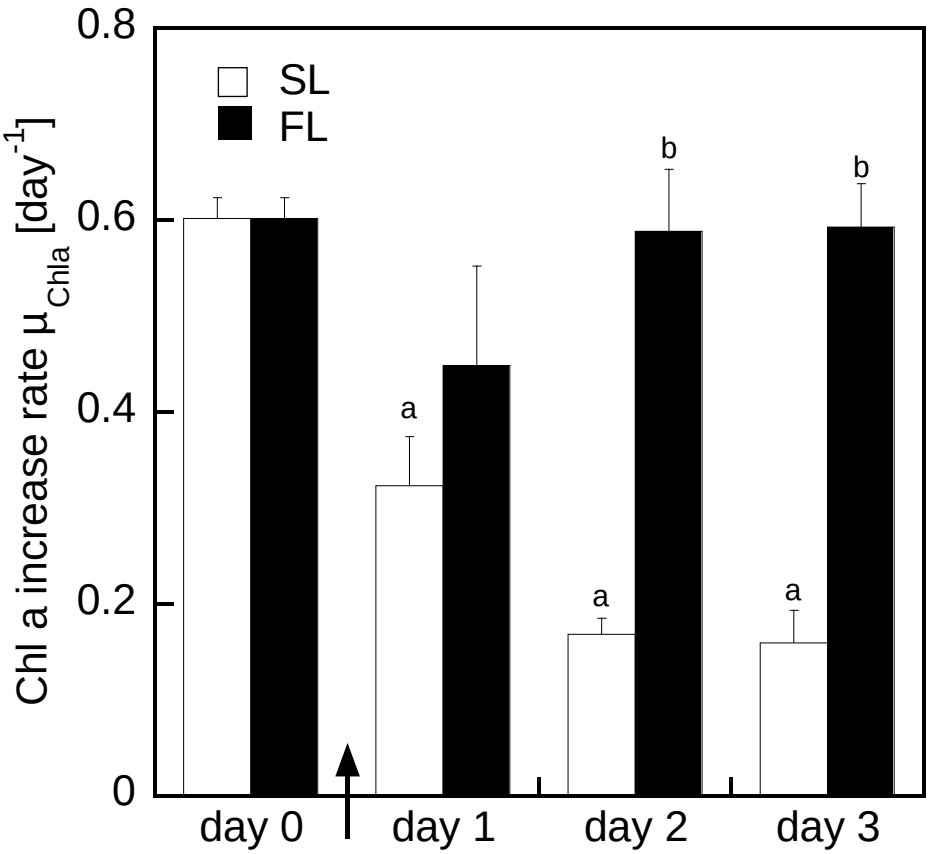

Lepetit et al., Fig. 6

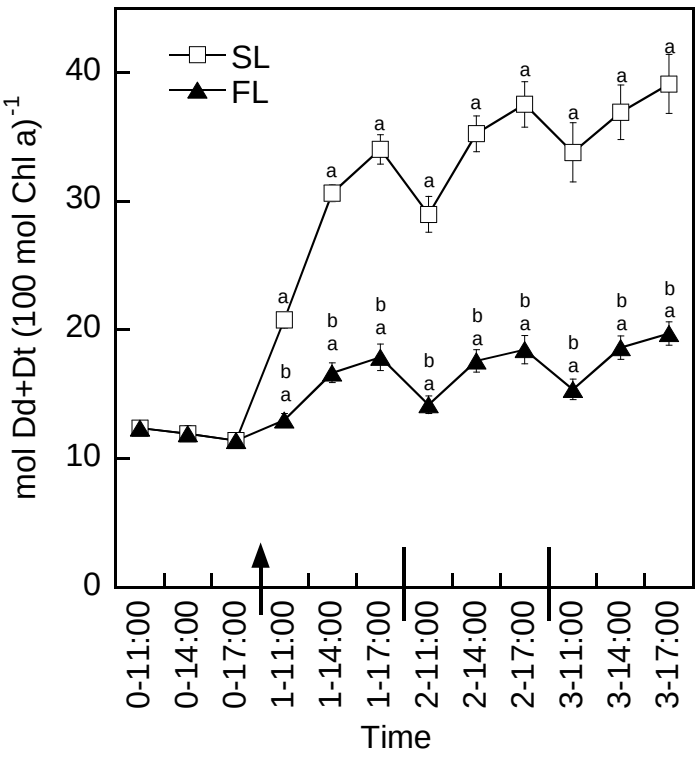

Lepetit et al., Fig. 7

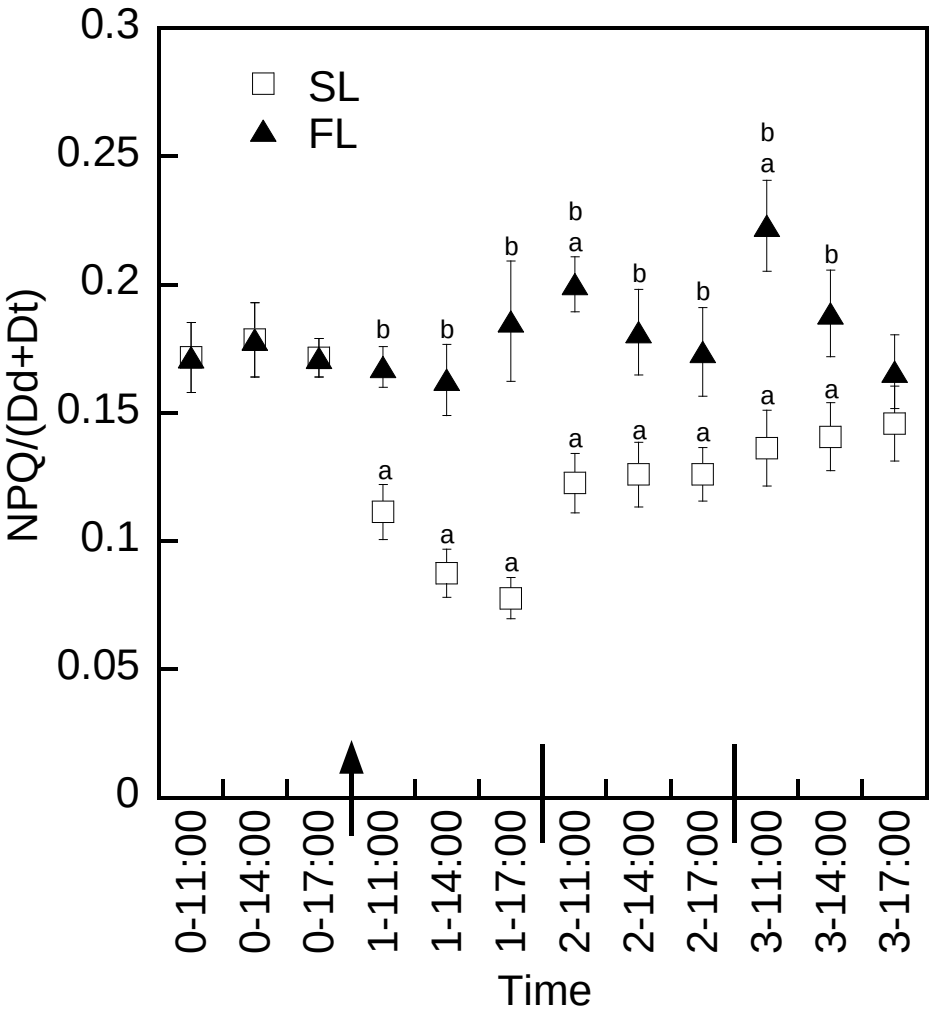

Lepetit et al., Fig. 8

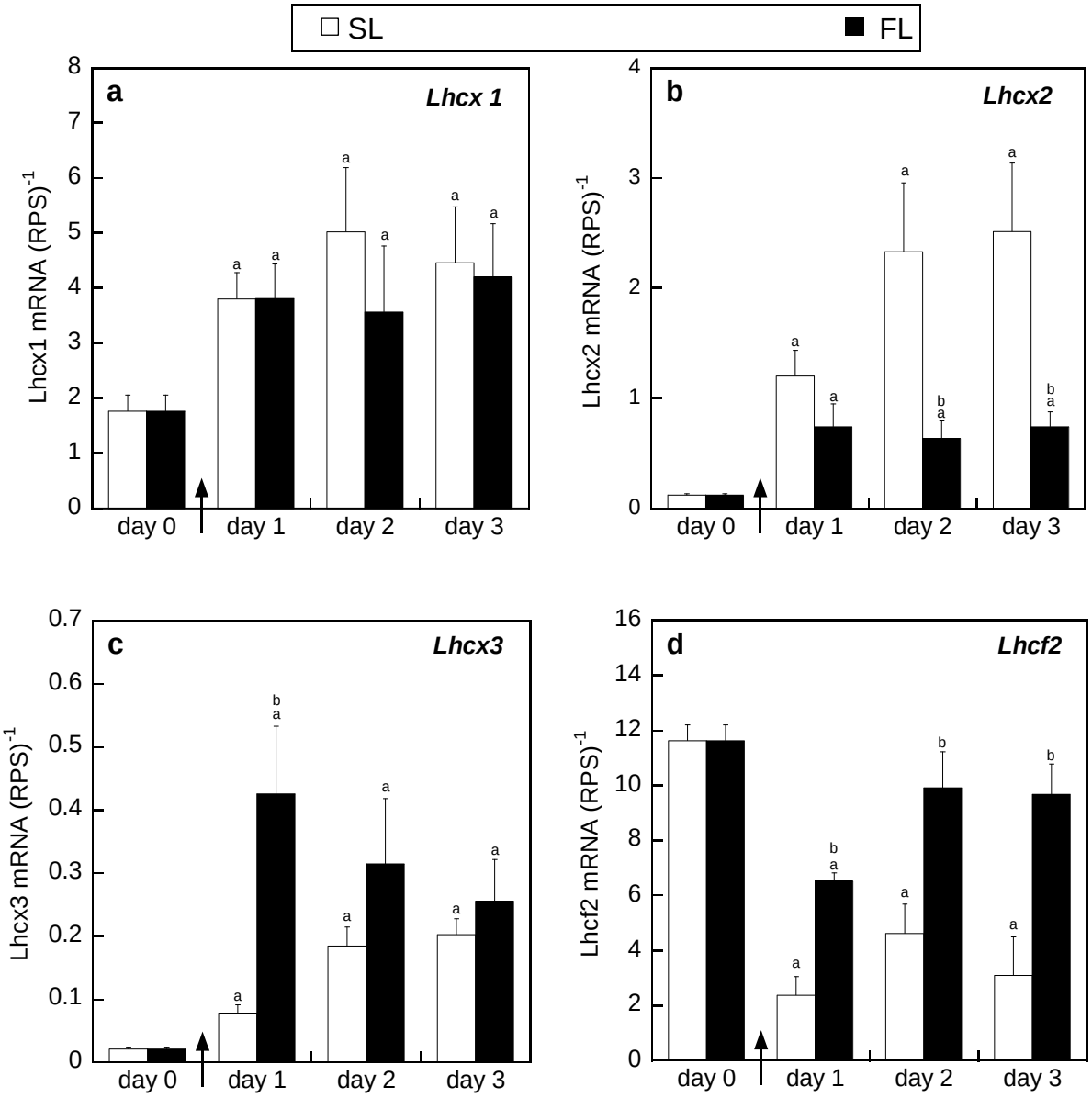

Lepetit et al., Fig. 9

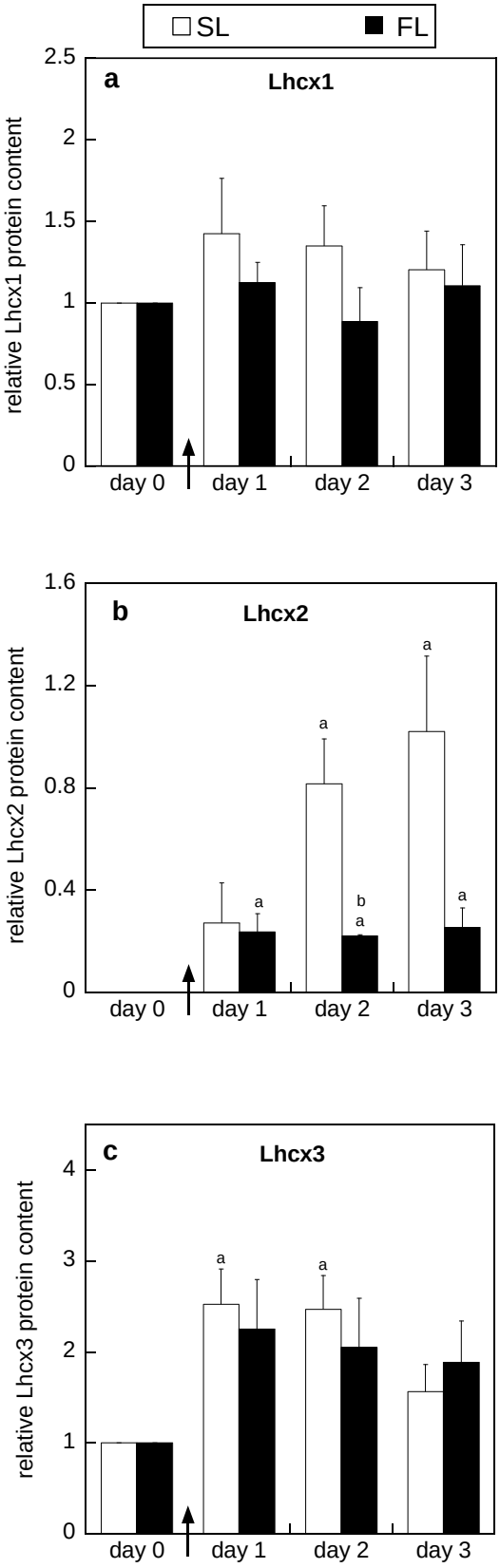

Lepetit et al., Fig. 10